

OPEN ACCESS

VUV irradiation studies of plasmid DNA in aqueous solution

To cite this article: M A Śmialek *et al* 2008 *J. Phys.: Conf. Ser.* **101** 012020

View the [article online](#) for updates and enhancements.

You may also like

- [Initial studies of the directional reflectance changes in pressed and sintered PTFE diffusers following exposure to contamination and ionizing radiation](#)
G T Georgiev, J J Butler, K J Thome *et al.*
- [Characteristics of Phosphor Degradation in AC-Driven Plasma Display Panels](#)
Chang Hoon Ha, Bo Yong Han, Jae Soo Yoo *et al.*
- [Improvement of Luminescence Degradation of PDP Blue Phosphor with New UV Phosphor](#)
Nobuyuki Yokosawa, Go Sato and Eiichiro Nakazawa

PRIME
PACIFIC RIM MEETING
ON ELECTROCHEMICAL
AND SOLID STATE SCIENCE

HONOLULU, HI
Oct 6-11, 2024

Abstract submission deadline:
April 12, 2024

Learn more and submit!

Joint Meeting of
The Electrochemical Society
•
The Electrochemical Society of Japan
•
Korea Electrochemical Society

VUV irradiation studies of plasmid DNA in aqueous solution

M A Śmialek^{1,2}, S V Hoffmann³, M Folkard⁵, K M Prise⁴, D E G Shuker², N S Braithwaite¹ and N J Mason¹

¹ Department of Physics and Astronomy, The Open University, Walton Hall, Milton Keynes, MK7 6AA, UK

² Department of Chemistry and Analytical Sciences, The Open University, Walton Hall, Milton Keynes, MK7 6AA, UK

³ Institute for Storage Ring Facilities, University of Aarhus, Ny Munkegade, DK-8000 Aarhus C, Denmark

⁴ Centre for Cancer Research and Cell Biology, Queen's University Belfast, 97 Lisburn Road, Belfast, BT9 7BL

⁵ Gray Cancer Institute, PO BO Box100, Mount Vernon Hospital, Northwood, HA6 2JR, UK

E-mail: m.a.smialek@open.ac.uk

Abstract. Interactions of VUV light and DNA samples in aqueous solutions are reported. The damage induced by such radiation is quantified by monitoring both loss of supercoiled DNA and formation of single and double strand breaks using agarose gel electrophoresis. Irradiations were performed using synchrotron VUV photons of 130, 150, 170 and 190 nm. VUV irradiation experiments revealed enhanced damage upon irradiation with 170 nm photons as compared with irradiations with photons of 150 nm and 130 nm. Irradiations carried at 190 nm caused the least damage.

1. Introduction

The significance of DNA – UV interactions has been known for a long time and extensive studies have been undertaken to understand the mechanisms by which the VUV damages DNA and to investigate possible damage pathways.

The first studies of interactions of VUV-UV photons with dry DNA films were undertaken by Sontag and Dertinger [1]. It was shown that the survival of unbroken DNA after VUV irradiation was very low, whereas irradiation by UV around 260 nm, although highly absorbed, does not cause any damage. The data obtained correlated with their earlier work [2] on VUV-UV absorption of DNA films.

Later studies on the dinucleotides showed that the damage induced by VUV is bond selective [3, 4] and that the most efficient combination of the mononucleotides that can undergo disruption is the adenosine dimer. The authors also showed that all the investigated complexes decomposed to fragments containing 5'-deoxymononucleotides and that the minimum energy required to decompose this complex was 7.3 eV.

Irradiation studies of dry plasmid pBR322 have been carried out by Ito *et al.* [5] revealing that the cross section for SSB formation increases steadily from 200 nm up to 120 nm. It was suggested that

over such a wavelength range the cross section did not behave like the photoabsorption spectrum, i.e. lesion formation was not influenced by photoabsorption in the DNA bases.

In studies by Hieda *et al.* [6], solid films of plasmid DNA have been irradiated at photon energies ranging from 8.3 eV to 20.7 eV and the damage obtained was quantified to be 5.4 times greater for SSBs and 12 times greater for DSBs at 20.7 eV compared to 8.3 eV.

Dose – response experiments for dry plasmid DNA films were repeated by Michael *et al.* [7] with the photons ranging from 8 eV to 25 eV. A slow increase in both SSBs and DSBs yields below 10 eV was reported and a 12 to 20 fold difference between the yield of SSBs and DSBs for energies investigated. Additionally, all the responses obtained showed energy-dependent plateaus at higher doses, which could have been caused by DNA shielding. They also suggested that to irradiate plasmid DNA in the aqueous solution would be more representative of the natural environment of DNA.

Irradiations of vacuum dried plasmid DNA were performed at 160 nm, 190 nm, 220 nm and 254 nm (Wehner *et al.*[8]) and it was concluded that the cross sections for SSB induction are $(1.5\pm 0.1)\times 10^{-17}$ cm², $(4.4\pm 0.6)\times 10^{-19}$ cm², $(5.0\pm 1.3)\times 10^{-19}$ cm² and $(2.1\pm 0.2)\times 10^{-19}$ cm², respectively. The authors conducted irradiations at 254 nm of DNA in aqueous solution and the air-dried plasmid. The cross sections obtained for the SSB formation were $(5.0\pm 0.4)\times 10^{-19}$ cm² and $(6.6\pm 1.0)\times 10^{-19}$ cm², respectively. The authors obtained the DSBs formation only for 160 nm with the cross section $(1.4\pm 0.1)\times 10^{-18}$ cm².

The first results obtained for an aqueous solution of plasmid DNA irradiated with photons of energy of 8 eV (Folkard *et al.*[9]) showed that there is a strong influence of the medium on the damage induced. Their preliminary results showed a high increase in the damage yield compared to the dry plasmid DNA. The authors showed that this was due to OH radical-induced damage by introducing the scavenger into the solution. The damage was halved with the scavenger present compared to the pure water solution. In later studies by Folkard *et al.*, [10] using 8.5 eV photons and ⁶⁰Co γ -rays the authors noticed little difference between the damage induced to plasmid DNA in aqueous solution by the two types of radiation. It was concluded from these experiments that all UV wavelengths that can be absorbed by water will induce damage to DNA, amount of which will depend on the yield of OH radicals.

2. Experimental apparatus, materials and methods

2.1. Apparatus

The experiments were performed at the synchrotron radiation source in Aarhus, Denmark. The setup used in the experiments is shown in Figure 1. After passing through the exit slit of the monochromator, the light illuminates the surface of a VUV detector. The VUV detector used for the photon flux measurements was a GaP VUV diode with an active surface of 10.9 mm², purchased from Roithner Laser Technik and calibrated over the VUV region (100 nm to 200 nm) at Physikalisch-Technischen Bundesanstalt (PTB), Germany.

Once the current was measured the irradiation time necessary for a desired dose was obtained and a sample was placed in the former position of the UV detector. The wet cell that allows for irradiation of plasmid DNA in aqueous solution with VUV photons of wavelengths of 110 nm and longer, presented in Figure 2, was previously described in [9] and used in later studies [10].

Rotation of the sample during irradiation allows for the uniform mixing of the material, so all the molecules can reach the area of the VUV light penetration (typically a fraction of a micron in water). Rotation also prevents local overheating of the sample and thus reduces the amount of damage caused by direct heating of the DNA sample.

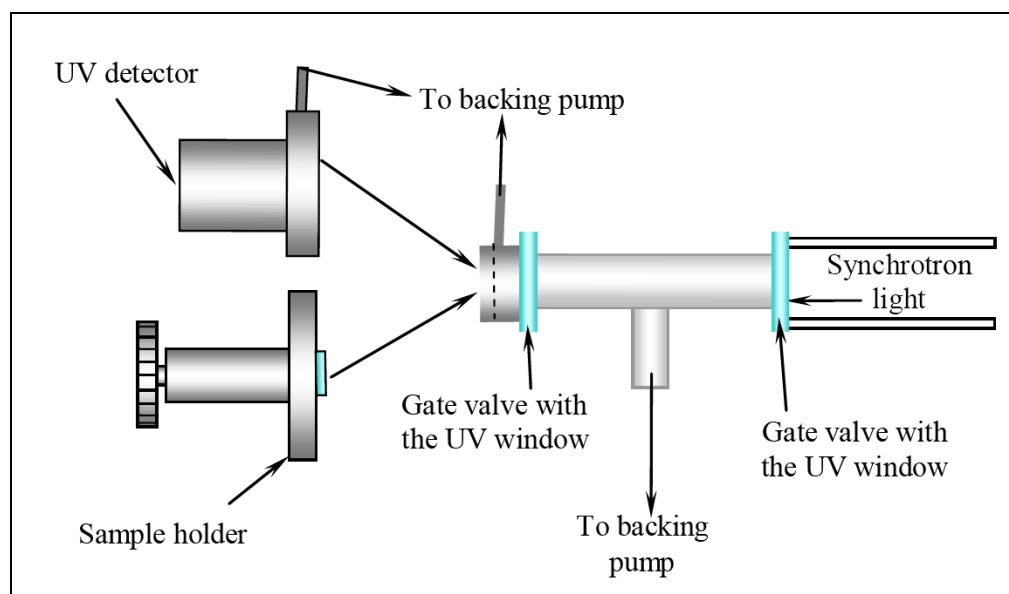


Figure 1. Experimental setup used on the synchrotron to irradiate DNA samples in aqueous solutions.

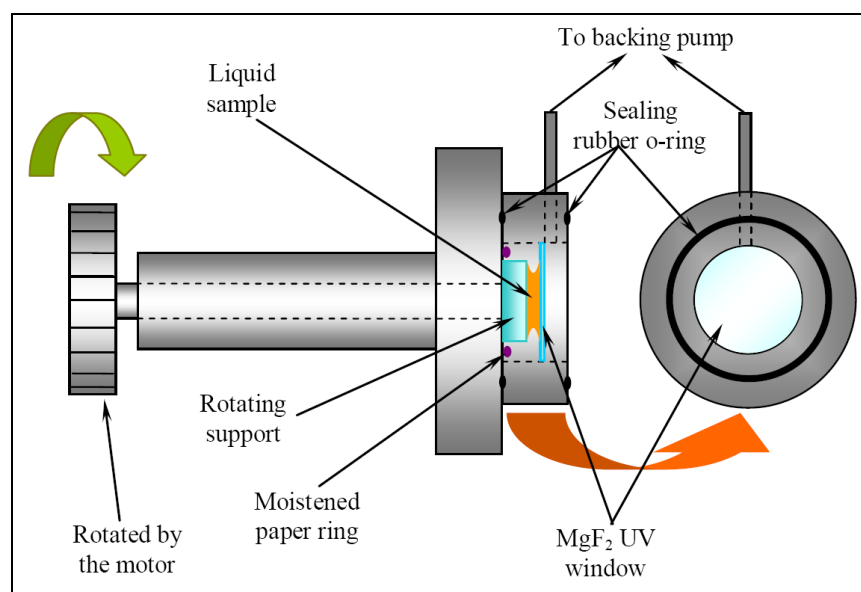


Figure 2. Schematic diagram of the wet cell with the sample in place.

2.2. Materials and methods

For all the irradiation experiments described in this chapter plasmid pBR322 DNA samples were prepared using commercially available kit for plasmid purification from Qiagen. Samples were eluted into pure water. The plasmid concentration varied from ~ 150 ng/ μ l to ~ 200 ng/ μ l. Samples were then placed in the sample holder shown in Figure 2 and irradiated as described above.

After irradiation small samples of irradiated product (2 μ l) were collected from the sample holder, diluted up to the volume of 5 μ l with tris buffer and either stored in the freezer awaiting further analysis or mixed with 2 μ l of loading buffer and run immediately on a 1.2 % agarose gel for 6 hours at 1.6 V/cm. Gels were then stained with 1 x SYBRGreenI solution in 1 x TBE buffer for 30 to 45

minutes. Fluorescent images of the gel were then recorded using commercial gel imagers and damage analysis was performed using ImageJ software (available from <http://rsb.info.nih.gov/ij/>).

In most cases sample recovery from the sample holder measured by AGE was close to 100%, therefore the assumption was made that no multistrand breaks are induced upon the irradiations over VUV-UV range. The loss of the material occurred only in cases where samples were irradiated for a very long time (i.e. above 4 hours) and was associated with the interaction between the glass support and DNA molecules.

2.3. Dose and irradiation time calculations

A set of DNA irradiations was performed to obtain dose response curves at certain photon energies. The absorbed dose, D_{absorbed} , is given by

$$D_{\text{absorbed}} = \frac{D}{[\text{sec}]} = \frac{h \cdot c \cdot I_{el} \cdot \Delta S}{\lambda \cdot M \cdot q_e \cdot Q_E \cdot s_{\text{det}}}, \quad (1)$$

where h is Planck's constant, c is speed of light, λ is wavelength [m], I_{el} is electron current on the UV detector [A], M is sample mass [kg], S is surface of the sample [mm²], s_{det} is surface area of the UV detector [mm²], q_e is electron charge, Q_E is quantum efficiency of the UV detector.

The time (number of seconds) needed for irradiation to reach the required dose can then be derived as

$$[\text{sec}] = \frac{D \cdot \lambda \cdot M \cdot q_e \cdot Q_E \cdot s_{\text{det}}}{h \cdot c \cdot I_{el} \cdot \Delta S}. \quad (2)$$

Cross sections for loss of supercoiled DNA were calculated using the following expression

$$\sigma_S(\lambda) = \frac{N_S}{N_{0S}} \cdot \frac{s_{\text{det}} \cdot Q_E \cdot q_e}{I_{el} \cdot T_{\text{irr}}}, \quad (3)$$

where $\sigma_X(\lambda)$ is the cross section for wavelength λ for loss of the supercoiled DNA, N_S is the remaining supercoiled DNA after irradiation, N_{0S} is amount of the supercoiled DNA form in the non-irradiated sample, T_{irr} is total time of irradiation [sec].

The expression can also be written as

$$\sigma_S(\lambda) = \frac{N_S}{D} \cdot \frac{h \cdot c \cdot \Delta S}{N_{0S} \cdot \lambda \cdot M}. \quad (4)$$

Such rearrangement will allow for further data modelling

3. Results and discussion

3.1. Supercoiled DNA loss and DSBs formation

Plasmid DNA was irradiated at 130 nm, 150 nm, 170 nm and 190 nm and the dose-response curves were measured. The rotation speed of the sample holder used in these experiments was set to be 1 revolution per second.

Figure 3 and Figure 4 present data obtained for the loss of the supercoiled DNA with increasing dose, whereas Figure 5 and Figure 6 show DSBs formation under the same conditions. The lines in Figure 3, Figure 4, Figure 5 and Figure 6 are linear fits to the data points and should be treated more as a guide to eye. The error bars represent the standard deviation between data points obtained experimentally in at least three independent irradiations.

The smallest amount of damage and hence smallest loss of the supercoiled DNA was found using 190 nm radiation. Surprisingly the damage at 130 nm was almost the same as that obtained for 150 nm, whereas the amount of DNA damage was greatest at 170 nm.

It was possible to observe DSBs for irradiations carried at all investigated wavelengths, although due to the large statistical variations in the experimental data it was hard to make any significant analysis of the data.

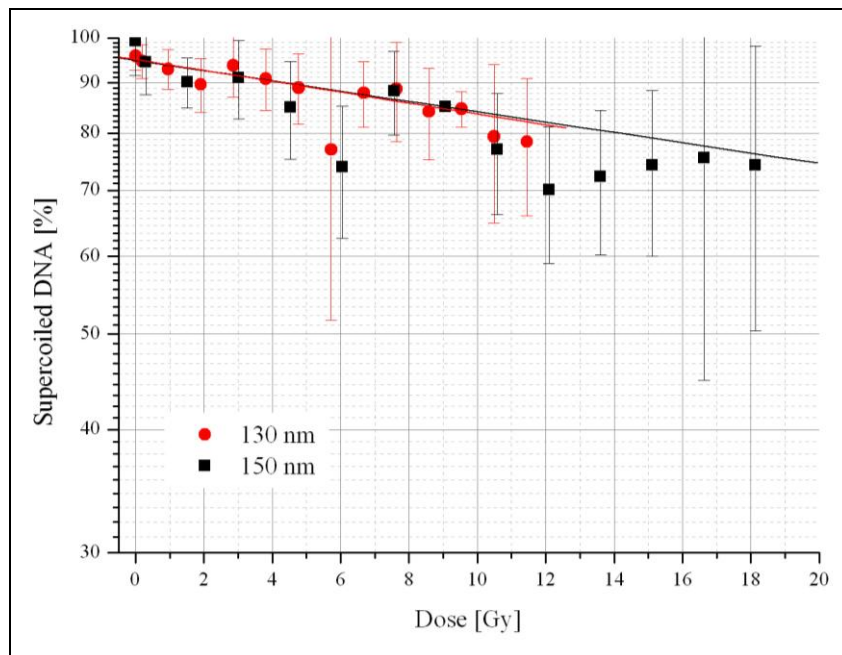


Figure 3. Dose-response curves for the loss of supercoiled DNA for plasmid samples irradiated at 130 nm and 150 nm; the lines represent a linear fit to the data.

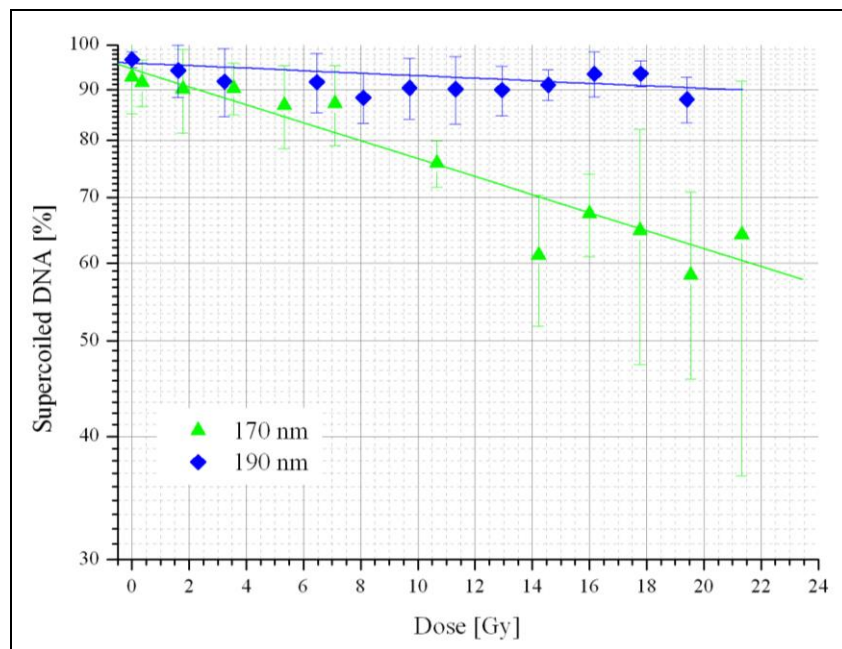


Figure 4. Dose-response curves for the loss of supercoiled DNA for plasmid samples irradiated at 170 nm and 190 nm; the lines represent a linear fit to the data.



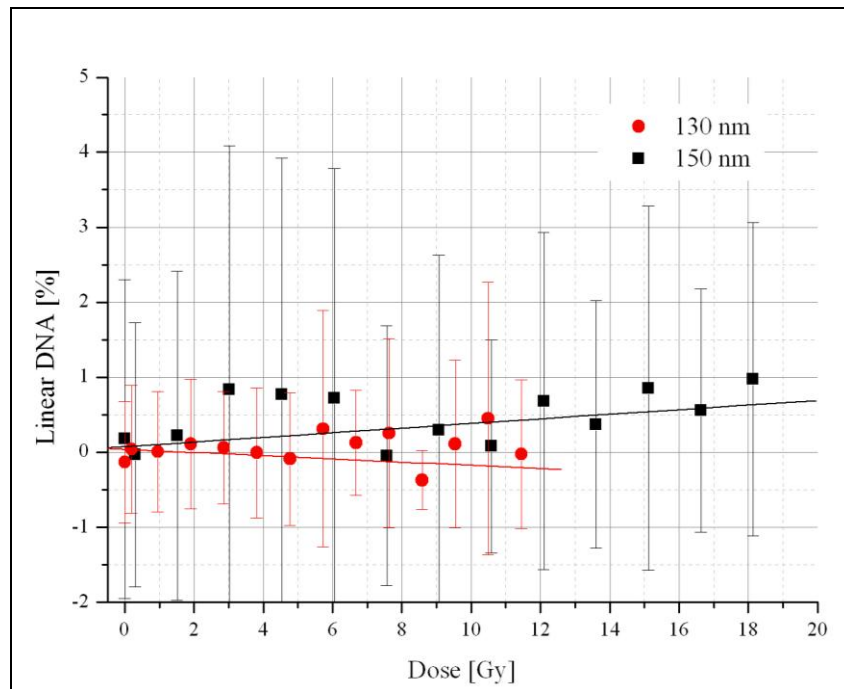


Figure 5. Dose-response curves for the DSBs for plasmid samples irradiated at 130 nm and 150 nm; the lines represent a linear fit to the data.

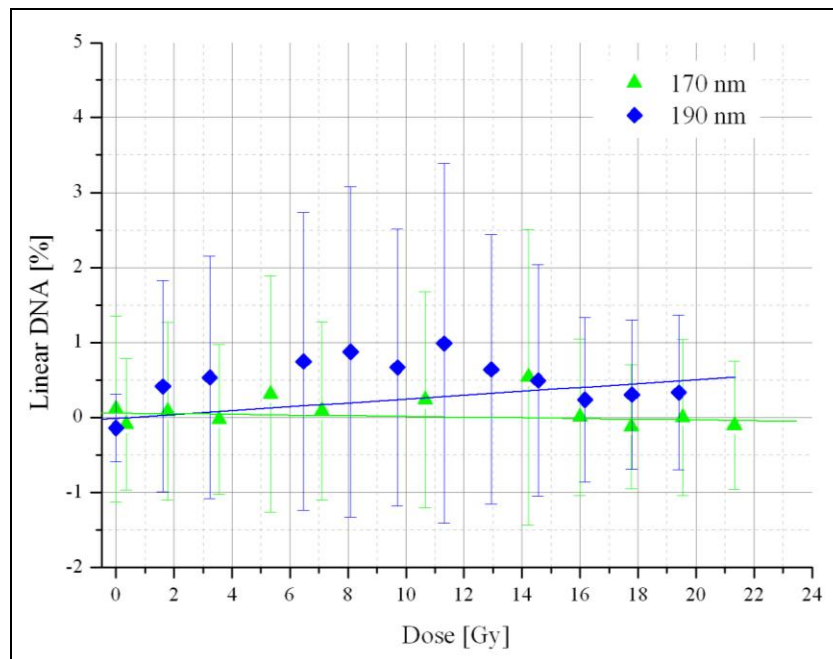


Figure 6. Dose-response curves for the DSBs for plasmid samples irradiated at 170 nm and 190 nm; the lines represent the linear fit to the data.

3.2. Cross sections calculations

Cross sections for loss of supercoiled DNA, σ_s , were derived using the measured data. Using equation (3), dose-dependent graph was obtained. Figure 7, presents the cross sections for loss of the supercoiled DNA at 130 nm, 150 nm, 170 nm and 190 nm. The estimated error was based on the standard deviation obtained for each point from AGE $\pm 20\%$ for the loss of the supercoiled DNA. As the cross sections errors for SSB and DSB were $\pm 150\%$ for SSB formation and $\pm 300\%$ for DSBs, that data was not analysed. Such high error values for the SSBs and DSBs formation cross sections were due to uncertainties whether the loss of the supercoiled DNA form will result in SSB or in DSBs. From the statistical distribution of these points (i.e. the values of standard deviation) one can deduce that their appearance is random.

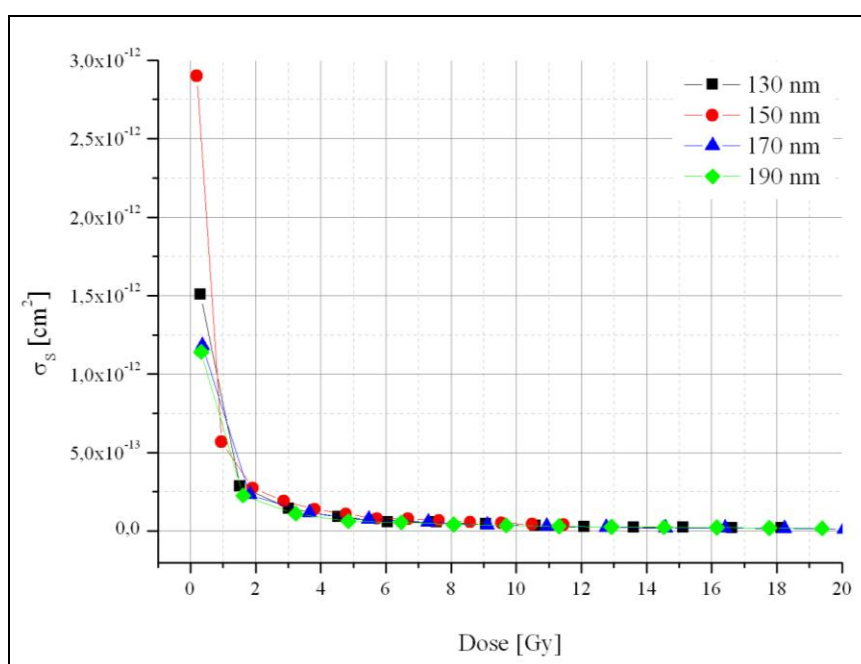


Figure 7. Cross section for loss of supercoiled DNA as a function of dose at 130 nm, 150 nm, 170 nm and 190 nm.

To interpret the data in Figure 7 one needs to consider what the cross section for the DNA damage means in this instance. In general the cross section describes the probability of an interaction between a projectile and a target in terms of the virtual size of the target. Therefore if the projectiles are small and subject to a low flux and yet the event occurred, the virtual size of the target must be big to ensure the interaction. This is nicely illustrated by the data presented in Figure 7. At low doses, below 2 Gy, where the amount of photons targeting the sample is small, the virtual size of the DNA molecule (i.e. the cross section) is large to ensure that that the event (i.e. damage) will occur. As the amount of photons targeting the sample increases (i.e. the dose increases), the cross section value decreases, as the probability of the interaction of photons with DNA molecules in such conditions is much greater. The slow decrease in the cross section as a function of dose reflects the nature of damage formation, namely the amount of supercoiled DNA in the sample decreases exponentially with radiation dose.

3.3. Data modelling

The derived cross sections were fitted using Microcal Origin 6.0 to a function of the form given by (4). Due to large errors the function was fitted only on the cross section values without taking into account the uncertainties. The cross section for the loss of supercoiled DNA was fitted with exponential, σ_s^E , function of the form

$$\sigma_S^E(\lambda) = P_1 \frac{P_2 \cdot e^{-P_3 \cdot D} + P_4}{D}$$

where:

$$P_1 = \frac{h \cdot c \cdot \Delta S}{\lambda \cdot M \cdot N_{0S}}$$

and P_2 , P_3 , and P_4 were determined by the fitting procedure. Term $P_2 \cdot e^{-P_3 \cdot D} + P_4$ describes loss of the supercoiled DNA form that was shown in Figure 3 and Figure 4.

In Figure 8 the fitted cross sections, based on the exponential function, are shown in detail. The cross section for loss of supercoiled DNA at 170 nm has a smaller value than the one for the damage at 150 nm (see the inserts in Figure 8) through the whole dose range, but it shifts of the original trend to higher values. None of the other fitted lines change their positions with respect to the other ones.

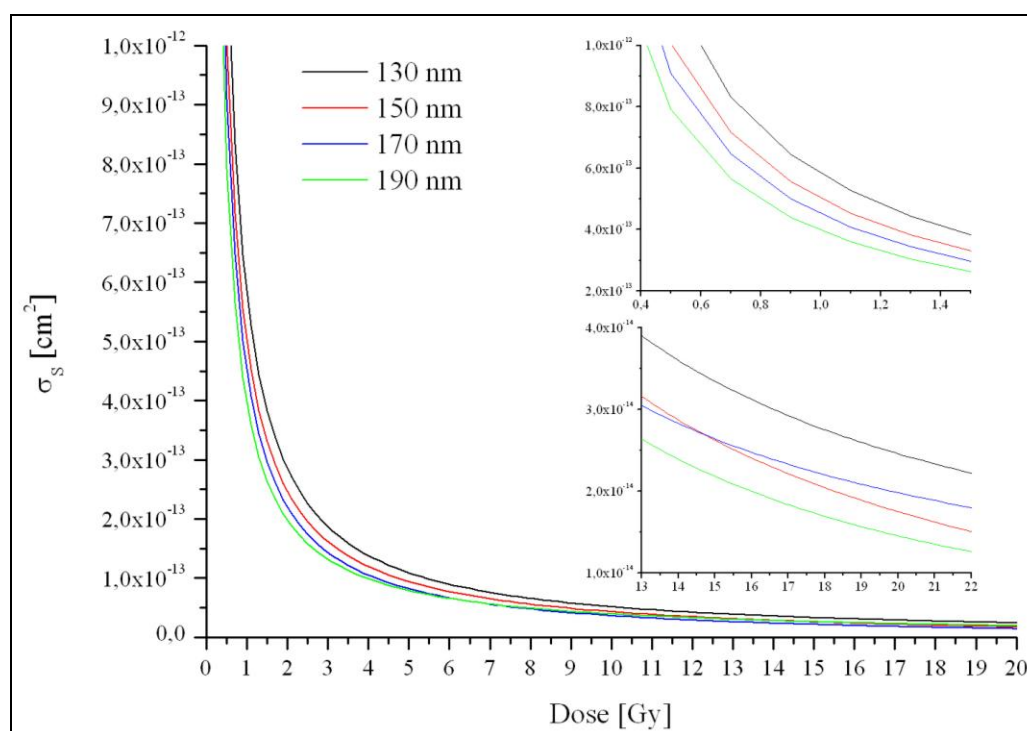


Figure 8. Fitted cross sections for supercoiled DNA loss.

The exponential functions obtained from fitting were used to model the behaviour of the supercoiled DNA loss. Figure 9 shows the trend lines obtained using that method. The fitted curves for 130 nm, 150 nm and 190 nm irradiations show similar trends. Damage obtained for irradiations carried at 170 nm, although fitted with the same type of function, expresses a different tendency, suggesting a constant increase in the loss of supercoiled DNA form with the applied dose.

Data shown in Figure 9 supports the assumption made in the beginning that the greatest damage can be obtained at 170 nm. Comparing to the cross sections shown in Figure 8, the damage at 170 nm is smaller than damage at 130 nm and 150 nm for the first 10 Gy delivered to the sample during irradiation. Due to a different trend in the function describing DNA loss at 170 nm, the damage at 170 nm increases continuously with the increasing dose delivered to the sample. Irradiations carried at 190 nm, 150 nm and 130 nm show more rapid supercoiled DNA loss at low doses, below 10 Gy, and more steady trends at higher doses.

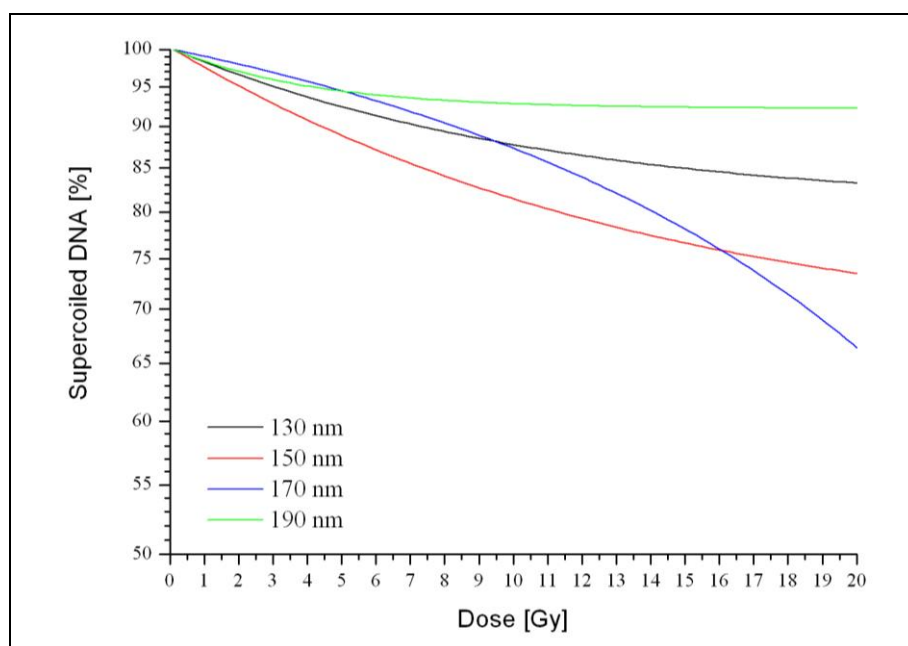


Figure 9. Comparison of the exponentially fitted trend lines for the loss of supercoiled DNA.

4. Conclusions

The data presented in this paper are consistent within the experimental error with the previous published results studying DNA damage in aqueous solution [10].

From an analysis of the data one can conclude that there is a decrease in the DNA damage yield with the increasing wavelength of radiation. Whilst one would expect the amount of damage to decrease with increasing wavelength, we found that damage is enhanced at 170 nm, whereas the amount of damage at 130 nm was almost the lowest of the four wavelengths investigated. The decrease in the damage produced at 130 nm can be ascribed both to the low penetration of photons of that energy and insufficient sample mixing over the irradiation periods as well as to the absorption of that energy by surrounding water. In case of the irradiations carried at 170 nm, a strong increase in the damage yield and abnormal tendency in the trend line obtained from data modelling occurred. This led to the conclusion that apart from the direct photon-induced damage there might be another process, like increased molecular absorption, taking place at this particular wavelength.

References

- [1] Sontag W and Dertinger H 1975 *Int. J. Radiat. Biol.* **27** 543
- [2] Sontag W and Weibezahn K F 1975 *Radiat. Environ. Biophys.* **12** 169-74
- [3] Ito T, Saito M and Taniguchi T 1987 *Photochem. Photobiol.* **46** 979-84
- [4] Ito T and Saito M 1988 *Photochem. Photobiol.* **48** 567-72
- [5] Ito T 1992 *Adv. Space Res.* **4** (4)249-53
- [6] Hieda K 1994 *Int. J. Radiat. Biol.* **66** 561-7
- [7] Michael B D, Prise K M, Folkard M, Vojnovic B, Brocklehurst B, Munro I H and Hopkirk A 1994 *Int. J. Radiat. Biol.* **66** 569-72
- [8] Wehner J, and Horneck G 1995 *Photochem. Photobiol. B* **28** 77-85
- [9] Folkard M, Prise K M, Brocklehurst B and Michael B D 1999 *J. Phys. B: Mol. Opt. Phys.* **32** 2753-61
- [10] Folkard M, Prise K M, Turner C J and Michael B D 2002 *Radiat. Prot. Dosim.* **99** 147-9